Title
Physiologic MRI for assessment of response to therapy and prognosis in glioblastoma

Journal
Neuro-Oncology, 18(4)

ISSN
1522-8517

Authors
Shiroishi, Mark S
Boxerman, Jerrold L
Pope, Whitney B

Publication Date
2016-04-01

DOI
10.1093/neuonc/nov179

Peer reviewed

Neuro-Oncology

Neuro-Oncology 18(4), 467–478, 2016
doi:10.1093/neuonc/nov179
Advance Access date 12 September 2015

Physiologic MRI for assessment of response to therapy and prognosis in glioblastoma

Mark S. Shiroishi, Jerrold L. Boxerman, and Whitney B. Pope

Department of Radiology, Keck School of Medicine, University of Southern California, Los Angeles, California (M.S.S.); Department of Diagnostic Imaging, Rhode Island Hospital and Alpert Medical School of Brown University, Providence, Rhode Island (J.L.B.); Department of Radiological Sciences, David Geffen School of Medicine at UCLA, Los Angeles, California (W.B.P.)

Corresponding Author: Whitney B. Pope, MD, PhD, Department of Radiological Sciences, David Geffen School of Medicine at UCLA, Los Angeles, California 90095 (wpope@mednet.ucla.edu).

Aside from bidimensional measurements from conventional contrast-enhanced MRI, there are no validated or FDA-qualified imaging biomarkers for high-grade gliomas. However, advanced functional MRI techniques, including perfusion- and diffusion-weighted MRI, have demonstrated much potential for determining prognosis, predicting therapeutic response, and assessing early treatment response. They may also prove useful for differentiating pseudoprogression from true progression after temozolomide chemoradiation and pseudoresponse from true response after anti-angiogenic therapy. This review will highlight recent developments using these techniques and emphasize the need for technical standardization and validation in prospective studies in order for these methods to become incorporated into standard-of-care imaging for brain tumor patients.

Keywords: diffusion, high-grade glioma, imaging biomarker, perfusion, physiologic imaging.

Pseudoprogression (PsP) and pseudoresponse remain substantial impediments to accurate response assessment of high-grade gliomas (HGGs). Advanced MRI may elucidate aspects of tumor physiology that augment structural information from conventional MRI when interpreting complex enhancement and fluid attenuated inversion recovery (FLAIR) signal changes in treated gliomas. Such physiologic techniques include diffusion and perfusion MRI, which have gained considerable experimental support as methods for improving diagnostic accuracy. Securing the potential gains in accuracy achieved with these techniques requires additional standardization and validation in prospective trials, with the overarching goal being the betterment of outcomes in HGG patients through improved clinical decision making. This review focuses on the latest advances in diffusion and perfusion MRI and provides an assessment of the evidence supporting the role of advanced MRI in improving the evaluation of HGGs.

Basic Principles of Perfusion and Diffusion MRI

Perfusion MRI

Brain perfusion can be assessed with MRI using dynamic susceptibility contrast (DSC), dynamic contrast-enhanced (DCE), and arterial spin labeling techniques. Because contrast-enhanced MRI is standard-of-care for assessing brain tumors, perfusion-weighted imaging (PWI) techniques using a gadolinium-based contrast agent (GBCA), particularly DSC-MRI and to a lesser extent DCE-MRI, are the most prevalent MRI-based methods for measuring brain tumor perfusion.[1–3] An overview of DSC- and DCE-MRI techniques is provided in Table 1.

DSC-MRI rapidly acquires gradient echo or spin echo planar images during first-pass transit through the brain of an exogenous, paramagnetic GBCA that transiently decreases signal intensity. Voxel-wise changes in contrast agent concentration are determined from signal-time curves and processed using tracer kinetic modeling and indicator dilution theory to estimate cerebral blood volume (CBV), cerebral blood flow (CBF), and mean transit time. Relative CBV (rCBV) is the most common DSC-MRI metric for evaluating brain tumors.

DSC-MRI is based on the assumption that a GBCA remains intravascular, a condition frequently violated in brain tumors. Various methods to minimize the error introduced by contrast extravasation have been developed, although no standardization of technique has yet been achieved.[4] A few options will be briefly discussed. One simple method is to focus analysis on nonenhancing portions of the tumor; however, this technique is obviously prone to bias and exclusion of the most malignant

Received 9 May 2015; accepted 1 August 2015

Table 1. Overview of DSC- and DCE-MRI

	DSC-MRI	DCE-MRI
Alternative names	Bolus-tracking MRI	Tl-weighted perfusion imaging, permeability imaging
Image weighting	T2/T2*	T1
Image acquisition	Rapid measurement of T2/T2*-weighted signal change before, during, and after bolus GBCA injection	Rapid measurement of T1-weighted signal change before, during, and after bolus GBCA injection
Common metrics in brain tumor imaging	rCBV	K^{trans}, v_p, v_e
Assumptions	Assumes GBCA remains within intravascular space; violation of this causes leakage effects, which is common in tumors and confounds rCBV measurements	Utilizes complex pharmacokinetic models to estimate microvascular permeability between intravascular space and EES

Abbreviations: EES, extravascular-extracellular space; K^{trans}, transfer constant; v_p, plasma space volume fraction; v_e, EES volume fraction.

contrast-enhancing portions of the brain tumor.[1] Other techniques include the use of gamma-variate fitting of the relaxivity-time curves to eliminate recirculation effects, and the use of low flip angles (ie, 35–60 degrees) or longer repetition times and echo times to reduce T1 contamination. However, one may encounter a lower signal-to-noise ratio of the CBV maps using these methods.[5,6] We recommend a technique which combines a preload of a GBCA along with model-based postprocessing leakage correction.[4,6] A preload refers to administration of a GBCA prior to the subsequent dose of a GBCA for the dynamic imaging in DSC-MRI. This, along with model-based postprocessing leakage correction, can decrease both T1 and T2* effects that can result in inaccurate rCBV values seen in enhancing lesions like brain tumors.

DCE-MRI is based on the T1 relaxivity properties of a GBCA. Whereas conventional contrast-enhanced MRI provides a qualitative, static depiction of brain tumor contrast enhancement, DCE-MRI quantifies various dynamic features of blood–brain barrier contrast agent leakage. Commonly, a 2-compartment (plasma and extravascular-extracellular spaces) pharmacokinetic model is used (Fig. 1).[7] After baseline T1 maps are obtained, T1-weighted DCE-MRI images are acquired before, during, and after a GBCA administration. A vascular input function is determined, and pharmacokinetic modeling yields the extravascular-extracellular (v_e) and plasma (v_p) space volume fractions, transfer constant (K^{trans}), and rate constant ($k_{ep} = K^{trans}/v_e$).[7] K^{trans}, thought to reflect microvascular permeability but also representative of blood flow and vessel surface area,[7] is the most common metric in brain tumor studies. The initial area under the contrast agent concentration curve (IAUC) is a model-free parameter reflecting CBF, CBV, microvascular permeability, and v_e that is less physiologically specific than K^{trans}.[7]

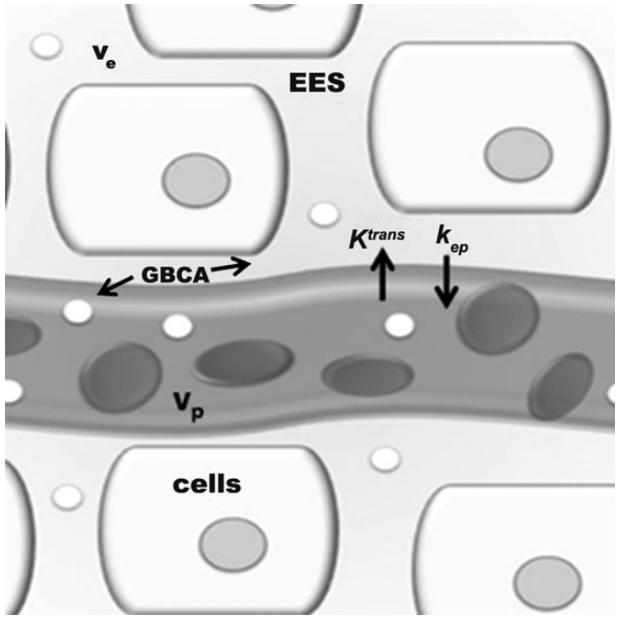

Fig. 1. Two-compartmental DCE-MRI pharmacokinetic model. A GBCA (circles) leaks across the vascular endothelium into the extravascular-extracellular space (EES) but does not enter into cells. K^{trans} represents the transfer constant between blood plasma and the EES, v_p is the plasma space volume fraction, v_e is the EES volume fraction, and k_{ep} is the rate constant (K^{trans}/v_e).

Diffusion MRI

Diffusion-weighted imaging (DWI) is sensitive to random microscopic (Brownian) motion of water molecules that results in signal loss and consequent hyperintensity in areas of restricted diffusion. The apparent diffusion coefficient (ADC) reflects the magnitude of water motion, with restricted diffusion having lower ADC values. DWI-based techniques can provide insight into the microscopic tissue environment, including intra- and extracellular space volumes. Increased extracellular water (as in vasogenic edema) increases ADC, whereas cytotoxic edema (from hypoxia or other causes of cell swelling) decreases ADC. More importantly for tumor imaging, ADC is inversely correlated with cell density,[8] probably due to reduced water mobility from dense cellular packing.

Functional diffusion maps (fDMs) are an extension of DWI in which coregistered scans from multiple time points are compared on a voxel-wise basis to temporally track stereospecific changes in ADC.[9] This permits visualization and quantification of regional variations of response within tumor and peritumoral regions, which is potentially significant in heterogeneous HGGs. Functional DMs require precise registration of images from

multiple time points, presenting a technical challenge. Ongoing work seeks to overcome this difficulty and improve the accuracy of fDM-based biomarkers by using innovative methods that quantify and reduce registration errors.[10]

Major Applications of Perfusion and Diffusion MRI to the Management of Brain Tumor Patients

PWI and DWI can augment conventional MRI in the initial-evaluation and posttreatment monitoring of brain tumors. Although there are many potential neuro-oncologic applications of these techniques, most fall within 4 distinct categories: (i) improving accuracy in prognosis and predicting efficacy of a specific therapy prior to treatment initiation; (ii) assessing efficacy of therapy before standard response indicators (eg, change in size of enhancing tumor) are affected; (iii) distinguishing true response from pseudoresponse and increasing sensitivity and specificity for nonenhancing tumor; and (iv) distinguishing true progression from PsP.

Determining Prognosis and Predicting Efficacy of Therapy Prior to Treatment

Several studies have demonstrated the prognostic value of rCBV in HGGs, finding that increased rCBV is associated with poorer outcomes. For instance, maximum rCBV within treatment-naive tumor correlates with OS,[11,12] and gliomas with mean rCBV >1.75 progress earlier than those with lower rCBV.[13] Similarly, high pretreatment baseline K^{trans} is associated with worse progression-free survival (PFS) and overall survival (OS).[14] A study combining DCE-MRI and DSC-MRI evaluations in the same newly diagnosed case of glioblastoma multiforme (GBM) found that both K^{trans} and rCBV correlated with OS.[15] Interestingly, K^{trans} and rCBV are typically not well correlated with each other,[16] suggesting that these perfusion metrics reflect different aspects of GBM biology.

In addition to use as a prognostic marker, PWI may also predict treatment response. A recent retrospective study of DCE-MRI in recurrent GBM found that baseline K^{trans} prior to bevacizumab treatment predicted PFS and OS.[17] Conversely, there was no relationship between pretreatment K^{trans} and outcome measures in a control cohort that did not receive bevacizumab therapy. This indicates that K^{trans} is a predictive, rather than prognostic, marker in this setting.

Similar to PWI, diffusion-based metrics also have both prognostic and predictive merit. For instance, in patients with HGGs treated with chemoradiation, low pretreatment mean tumor ADC is associated with shorter survival, potentially reflecting more cellular or aggressive tumor.[18,19] ADC histogram analysis improves upon mean diffusion metrics in characterizing the distribution of ADC values within areas of enhancement. Median values of the lower curve (ADC_L, thought to represent the tumor-rich rather than edematous/necrotic portion of the lesion) of double Gaussian fits of the histogram data predicted PFS and OS in bevacizumab-treated recurrent GBM. Specifically, higher ADC_L derived from pretreatment scans correlated with better outcomes following bevacizumab treatment, both in a single institution study[20] and in a multicenter trial.[21] ADC_L was not predictive of outcome following non–anti-angiogenic treatments, and thus ADC_L, similar to K^{trans}, may represent a predictive marker specific to bevacizumab or anti-angiogenic therapy. Similar results have been obtained for GBM treated with combined bevacizumab and sorafenib,[22] as well as using median ADC values in enhancing tumor,[23] further supporting the potential of DWI metrics to serve as predictive biomarkers.

The timing of bevacizumab treatment may impact the applicability of DWI biomarkers. For instance, unlike in the recurrent setting, higher ADC_L may not predict prolonged PFS or OS in newly diagnosed GBM patients treated with bevacizumab-containing regimens given with radiation therapy[24] and may even be associated with shorter PFS.[25] Recurrent and treatment-naïve GBM are genetically distinct. For example, recurrent GBM is often hypermutated and more likely to be of the mesenchymal phenotype.[26–28] Potentially these differences impact imaging biomarkers, rendering them dependent on the type and timing of treatment, as well as the time point in the patient's treatment course at which they are acquired.

Assessing Early Response to Therapy

Cytotoxic therapy. Relative CBV appears to be an early response marker for GBM treated with cytotoxic methods and may add value to assessment of disease status based on anatomic MRI.[29,30] For instance, >5% increase in rCBV 1 month after temozolomide chemoradiation correlates with poor OS, whereas changes in enhancing tumor volume do not.[31] Analogous to fDMs for DWI, parametric response maps (PRMs) of voxel-wise perfusion changes stratify survival in HGGs treated with temozolomide chemoradiation.[9,32–34] Specifically, rCBV and rCBF PRMs from DSC-MRI 1–3 weeks after treatment were found to correlate with OS, while changes in mean rCBV or rCBF based on standard enhancing tumor region-of-interest (ROI) analysis did not.[35] Comparison of (i) percentage change of whole tumor rCBV, (ii) physiologic segmentation into low, medium, and high rCBV, and (iii) PRM applied to serial rCBV measurements at baseline and after 1 and 3 weeks of chemoradiation in GBM found that only PRMs predicted 1-year survival.[36]

Based on the hypothesis that cell membrane destruction following cell death yields enhanced water movement and increased ADC that precede tumor shrinkage, fDM-based DWI has also been investigated as an early response marker following cytotoxic therapy. For example, brain tumors containing a significant proportion of voxels with increased ADC between baseline and 3 weeks post-chemoradiation have better response at 10-week MRI than tumors without a shift toward increased ADC,[9] and fDMs 10 weeks post-chemoradiation initiation predict 1-year survival in HGGs.[32,37] Functional DMs between baseline and post-temozolomide chemoradiation in GBM have also shown that large volumes of tumor with decreasing ADC portend shorter PFS and OS.[38,39] Similarly, the volume of GBM with decreased ADC on fDMs 2 days after boron neutron capture therapy, an alternative to standard radiation treatment, correlates with MRI-defined response at 10 weeks.[40] These results are supported by data from preclinical models using both cytotoxic chemotherapy[41] and radiotherapy,[42] demonstrating that tumors with increasing ADC on fDMs have increased cytotoxicity and better outcomes. Thus, there is emerging evidence that fDMs can augment standard MRI as an

early response marker following irradiation alone or in combination with cytotoxic chemotherapy.

Anti-angiogenic therapy. Theoretically, the microvascular sensitivity of PWI should have utility for assessing response to anti-angiogenic therapy. However, a retrospective study of bevacizumab-treated recurrent GBM found only marginally significant association of change in rCBV between baseline and first follow-up and time to progression.[43] Similarly, early post-treatment changes in K^{trans} and rCBV were not predictive of OS in recurrent HGGs treated with both bevacizumab and temozolomide.[44] However, more promising results were recently obtained using leakage correction and a method for standardizing rCBV measurements across MR scanners and field strengths to predict response to bevacizumab in recurrent HGGs.[45] Standardized rCBV measured 60 days before and 20–60 days after bevacizumab therapy was predictive of PFS and OS, while FLAIR hyperintense and contrast-enhancing volumes were not. Additionally, using a population-based rCBV atlas to minimize bias resulting from rCBV variability, pre- and post-bevacizumab hypervascular rCBV volumes in recurrent GBM were predictive of PFS and OS, whereas traditional PWI measures including mean and maximum rCBV were not.[46] And recent results from American College of Radiology Imaging Network (ACRIN) 6677/Radiation Therapy Oncology Group (RTOG) 0625, a multicenter, randomized, phase II trial of bevacizumab with irinotecan or temozolomide in GBM, demonstrated that increasing rCBV between baseline and 2 or 16 weeks post-bevacizumab initiation portends worse OS.[47] Therefore, there is emerging evidence that DSC-MRI can help prognosticate OS and PFS shortly after treatment initiation with bevacizumab.

As with cytotoxic therapy, fDMs and ADC histogram analysis have provided early response markers for anti-angiogenic therapy.[10,48–50] For instance, fDMs derived from pretreatment and 6-week post-bevacizumab initiation scans stratified PFS and OS in a cohort of recurrent GBM using ROIs defined within contrast-enhancing or abnormal FLAIR regions.[10] Nonlinear registration of ADC maps for fDM generation improved the prognostic value, and relatively high sensitivity (64%) and specificity (73%) for 6-month PFS using ROIs defined by abnormal FLAIR hyperintensity were realized. In addition to nonlinear registration, graded fDMs, in which change in ADC is segmented into discrete bins, also better predicted OS than standard fDM approaches.[49] Furthermore, in a study of pre- and post-bevacizumab-treated recurrent GBM, baseline ADC parameters within nonenhancing FLAIR hyperintensity and subsequent changes in ADC within enhancing tumor between pre- and posttherapy scans stratified OS and PFS.[48]

As mentioned, the timing of anti-angiogenic therapy impacts DWI-based biomarkers. For instance, traditional and graded fDM metrics appear less predictive of outcomes when applied to patients receiving up-front as opposed to adjuvant bevacizumab.[24] Changes in ADC from mid- to post-radiotherapy appear to outperform changes from pre- to mid-radiotherapy or pre- to post-radiotherapy.[51] These results are particularly notable given that mid-radiotherapy scans are typically not acquired in standard patient treatment regimens, even though they may contain useful prognostic information.

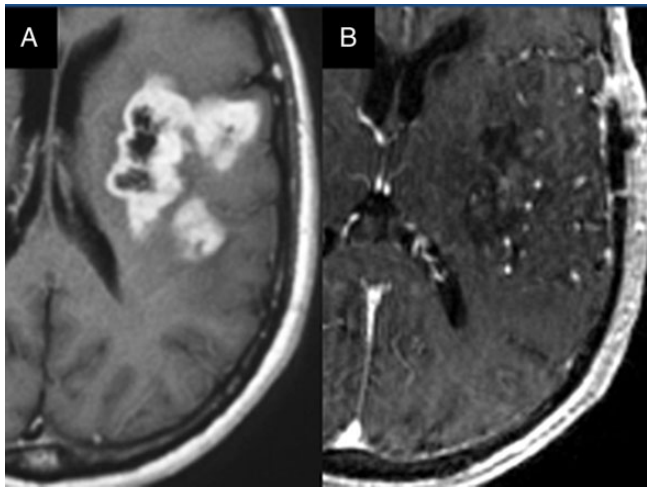

Fig. 2. Pseudoresponse. Contrast-enhanced axial T1-weighted MRIs of a recurrent GBM tumor before (A) and after (B) bevacizumab therapy demonstrate a marked decrease in the amount of contrast enhancement 6 days following initiation of anti-angiogenic therapy.

Distinguishing Response from Pseudoresponse and Detection of Nonenhancing Tumor

Anti-angiogenic therapy "normalizes" the blood–brain barrier, diminishing transvascular gadolinium leakage and contrast enhancement. This can result in "pseudoresponse," which reflects decreased contrast enhancement independent of antitumor effect and likely accounts for the high response rate and prolonged PFS without improved OS in bevacizumab-treated GBM (Fig. 2).[52] Similar shortcomings of conventional imaging have been demonstrated in other studies,[53,54] posing a limitation for early response assessment and leading to inclusion of FLAIR-based nonenhancing tumor in modified response assessment criteria.[55]

Identification of nonenhancing tumor, however, remains challenging. Bevacizumab treatment can result in a marked decrease in vasogenic edema, and although increasing FLAIR hyperintensity following bevacizumab treatment often represents nonenhancing tumor, other common entities such as persistent vasogenic edema and gliosis can mimic or mask nonenhancing tumor, degrading specificity (Fig. 3). The role of contrast enhancement and FLAIR in predicting OS has been controversial. This is exemplified in recent results from ACRIN 6677,[56] where, not surprisingly, patients with progressive enhancement after 2 or 4 anti-angiogenic therapy cycles had significantly shorter OS than nonprogressors. However, there was no survival benefit for patients with improved versus stable enhancement, likely due to pseudoresponse. Furthermore, there was no survival prognostication with FLAIR, suggesting that conventional imaging fails to stratify OS for anti-angiogenic therapy.

DSC-MRI may help identify pseudoresponse and predict relative treatment success shortly after initiation of anti-angiogenic therapy. The ACRIN 6677 trial demonstrated significant OS differences for patients with increased versus decreased rCBV within enhancing tumor at 2 or 16 weeks posttreatment initiation compared with baseline.[47] Furthermore, DSC-MRI successfully

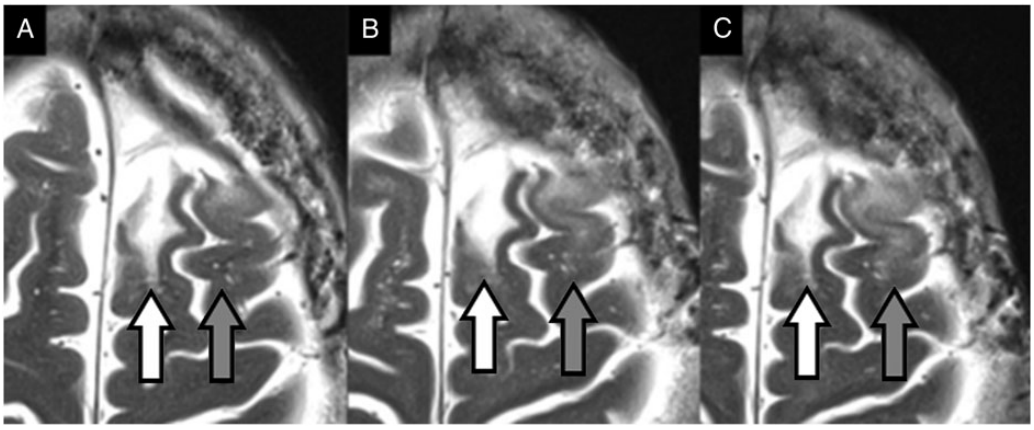

Fig. 3. Possible nonenhancing tumor vs gliosis or edema. Axial T2-weighted images following surgical resection and chemoradiation (white arrows) of a left frontal anaplastic astrocytoma (A) with follow-up imaging performed 1 year (B) and 1-1/2 years (C) later demonstrate a slight increase in the amount of T2 hyperintensity along the lateral margin of the resection site (darker arrow in C), which may represent gliosis or edema. However, nonenhancing recurrent tumor cannot be excluded.

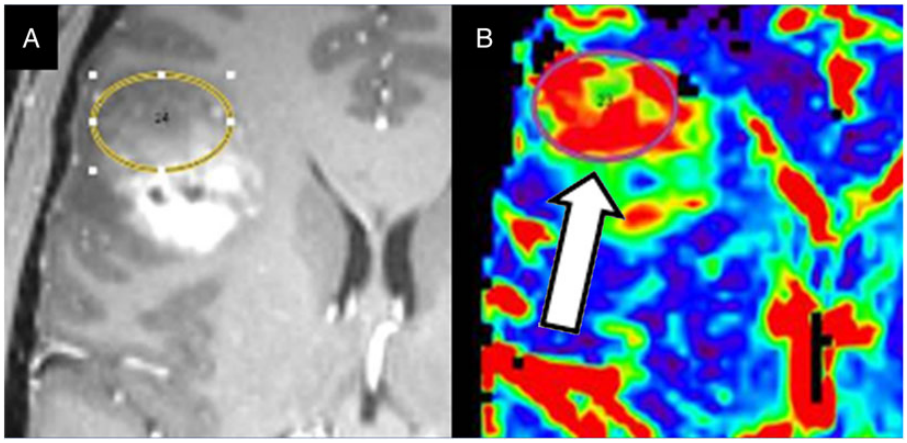

Fig. 4. DSC-MRI and nonenhancing tumor. Contrast-enhanced axial T1-weighted MRI (A) and color rCBV map (B) from DSC-MRI demonstrate a nonenhancing region (yellow oval, A) along the anterior aspect of an enhancing right-sided GBM with increased rCBV (white arrow, B), consistent with nonenhancing tumor.

substratified the nonprogressors on conventional T1-weighted postcontrast MRI. Whereas there was no survival difference between T1 responders and patients with stable disease, OS was significantly longer for patients with decreased rather than increased rCBV at 2 weeks compared with baseline, suggesting that DSC-MRI can identify likely relative treatment successes.[57] Early posttreatment standardized rCBV also predicted OS and PFS in a similar single-institution study of 36 recurrent HGGs imaged with DSC-MRI 20–60 days after bevacizumab.[45]

Results such as these may motivate an interpretation paradigm for recurrent GBM shortly after bevacizumab whereby patients with progressive contrast enhancement are deemed treatment failures, but instead of using responsive enhancement status for further substratification, change in rCBV would be used to further distinguish relative treatment successes from failures. Larger prospective trials are warranted.

PWI may also improve identification of nonenhancing tumor by diminishing the nonspecificity of FLAIR signal changes. Multiparametric DCE-MRI and DSC-MRI methods applied to nonenhancing regions indicate that decreased rCBV and rCBF and absence of increased K^{trans} in bevacizumab-treated GBM distinguish vasogenic edema from infiltrative tumor and correlate with PFS.[58,59] Principal component analysis of temporal DSC-MRI data in GBM identify peritumoral regions likely to be infiltrated with tumor and correlate with OS.[60] And increasing rCBV in nonenhancing peritumoral and transcallosal regions has been shown to associate with poor OS (Fig. 4).[61] A multivariate model including KPS, age at diagnosis, and rCBV of nonenhancing regions found rCBV to be more prognostic than other imaging, genomic, or clinical features.

DWI has also been applied to GBM receiving with antiangiogenic therapy, based on the theory that lower ADC reflects higher cellularity and is more likely to be seen in tumor infiltration than vasogenic edema. The volume of FLAIR hyperintensity with abnormally low ADC that increases over time has been postulated to correspond with tumor infiltration,[62] and there is histopathological evidence to support this.[63] ADC histogram analysis of FLAIR hyperintense regions indicate that the

development of enhancing lesions is associated with a shift toward lower ADC values,[64] which can precede the appearance of contrast-enhancing tumor by an average of 3 months.[65] Thus ADC-based metrics appear to have potential as early indicators of tumor progression, even during bevacizumab-associated suppression of tumor angiogenesis, contrast enhancement, and vasogenic edema.[66]

One caveat to the application of DWI for identifying nonenhancing tumor is that lower ADC values do not always correlate with increasing tumor infiltration. Rather, very low and persistent diffusion restriction can be associated with nonviable tissue demonstrating atypical necrosis.[67–70] These lesions tend to be periventricular, slowly change over many months, and are associated with better, rather than poorer, survival (Fig. 5). Persistent restricted diffusion has also been reported for bevacizumab-treated metastases.[71] More broadly, this type of necrosis-associated restricted diffusion may be thought of as a type of treatment toxicity.[72] It is also important to note that bevacizumab can induce stroke-like lesions as early as 4–8 weeks after start of therapy.[69] Thus the interpretation of low ADC lesions in bevacizumab-treated gliomas must be made with caution.

Distinguishing Progression from Pseudoprogression

Pseudoprogression (PsP) represents transient increased contrast enhancement mimicking tumor progression and complicates response criteria for radiological progression (Fig. 6). Differentiation from progressive disease (PD) is important for avoiding premature trial failures and selecting timely alternative therapies. Its mechanism is incompletely understood[73] but involves increased vascular permeability with edema and contrast enhancement that are difficult to distinguish from PD with conventional MRI.[74] PWI and DWI have been proposed as useful adjunct imaging modalities for identifying PsP.

Although mean rCBV from DSC-MRI has consistently been shown to distinguish tumor and radiation necrosis in the setting of late-delayed progressive enhancement following radiation therapy,[75–77] its utility for distinguishing PsP from PD in the setting of early-delayed progressive enhancement following temozolomide chemoradiation is more uncertain. There are several possible times for interpreting new or progressive enhancement for chemoradiation-treated gliomas, including early posttreatment to predict future response and at initial progressive enhancement to distinguish PsP and PD.

For early posttreatment evaluation, change in rCBV between baseline and follow-up 1 month after completion of temozolomide chemoradiation stratified OS in a study of 36 GBM tumors, whereas bidimensional enhancement measurements did not. In those patients with progressive enhancement at 1 month, increased mean lesion rCBV corresponded with PD, and decreased mean lesion rCBV with PsP, with favorable receiver operating characteristic curve analysis (Fig. 7).[31] However, another study of 27 HGGs 3 weeks after chemoradiation using parametric response maps paradoxically found the converse to be true, with reduced rCBV in lesions destined for PD.[78] Thus the relationship between outcomes and changes in rCBV requires further investigation to clarify these potential discrepancies.

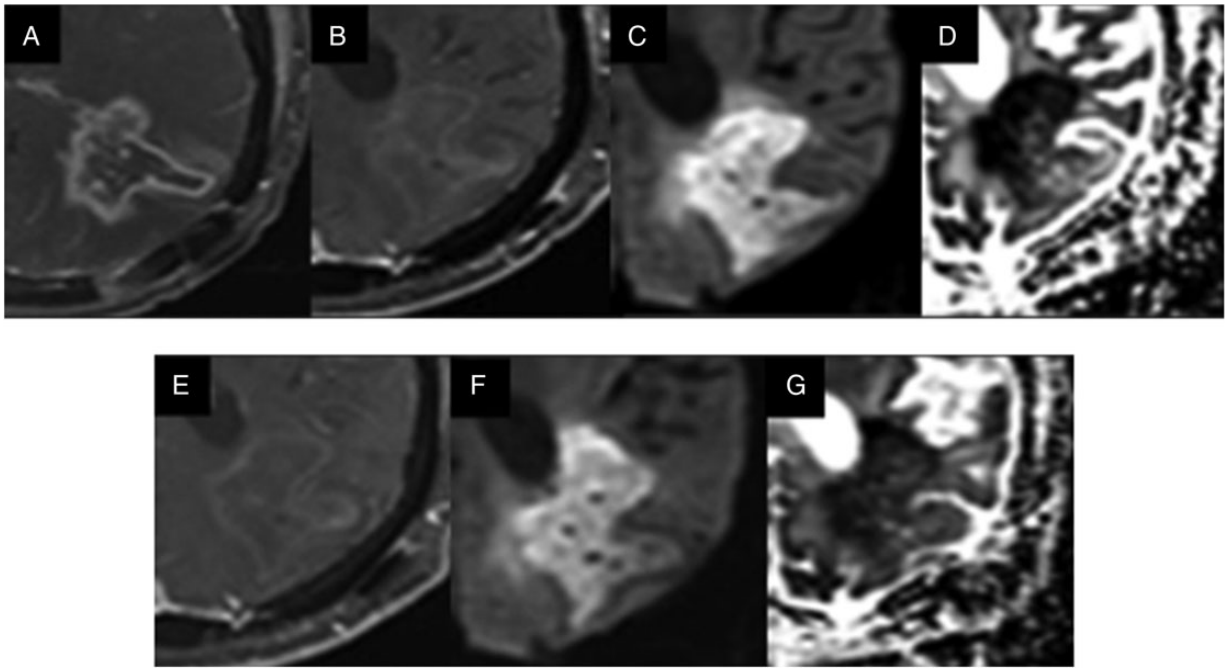

Fig. 5. Persistent diffusion restriction in recurrent GBM treated with bevacizumab. Contrast-enhanced axial T1-weighted image with fat saturation (A) demonstrates a necrotic, heterogeneously enhancing recurrent GBM in the left temporoparietal region. Follow-up imaging (B–D) after starting bevacizumab demonstrates marked decrease in contrast enhancement with development of prominent diffusion restriction (C, D: DWI and ADC map images, respectively). Another follow-up examination 2 months later (E–G) again demonstrates decreased contrast enhancement and persistent diffusion restriction.

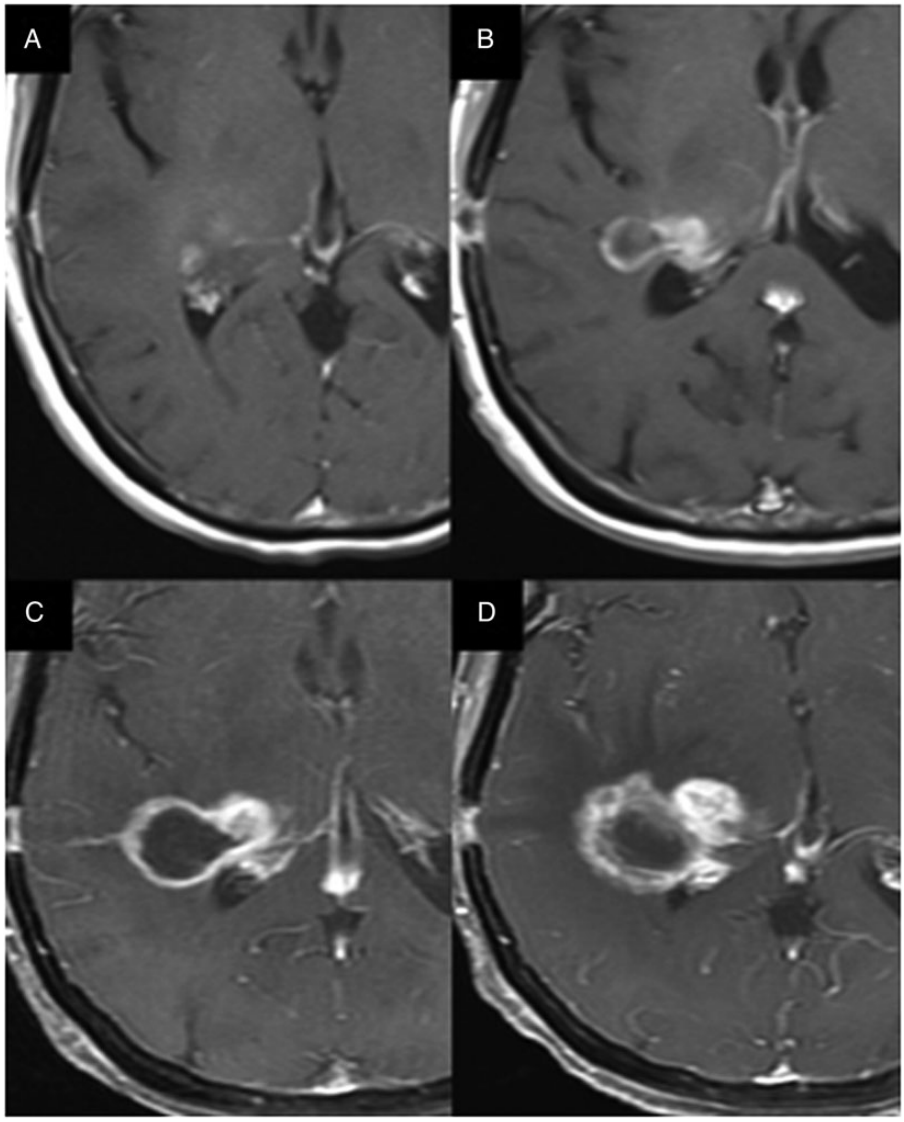

Fig. 6. Pseudoprogression vs true progressive disease. Axial contrast-enhanced T1-weighted image 2 days after biopsy (A) of a right thalamic HGG shows faint enhancement in the right thalamic region. Four weeks after temozolomide chemoradiation there is progressive enhancement (B) concerning for PsP vs true PD. After an additional 4 weeks, there is further progressive contrast enhancement (C). Follow-up after 4 more weeks (D) shows continued progressive contrast enhancement consistent with true PD rather than PsP.

Results are also conflicting for evaluation of disease status after initial progression of enhancement. Some studies have demonstrated significantly different median rCBV after temozolomide chemoradiation between PsP and PD using optimal thresholds of 1.3[79] and 1.8.[80] Another study found significant difference in mean rCBV, but only in GBM with unmethylated rather than methylated O^6-DNA methylguanine-methyltransferase.[81] To overcome limitations associated with contrast leakage in accurately determining rCBV, ferumoxytol, an intravascular iron-based agent not susceptible to leakage effects, has been employed and compared with a GBCA. In a pilot study of 14 GBM tumors at initial progressive post-chemoradiation enhancement, there was much better separation of mean rCBV between PD and PsP with ferumoxytol than with the GBCA.[82,83] Conversely, a retrospective study of HGGs treated with paclitaxel polyglumex, a powerful radiation sensitizer with a high incidence of profound PsP often coexistent with PD, found no significant difference in mean rCBV at initial progressive enhancement between lesions destined for PsP and PD.[84]

One possible explanation for these inconsistent results based on rCBV from a single time point for distinguishing PsP from PD is that coexistence of tumor and necrosis likely yields a spectrum of chemoradiation-induced vascular morphologies and potentially a wide range of vascular volumes.[85] Therefore, especially early in lesion evolution, mean rCBV may be inadequate for capturing the dominant tumor behavior. Conversely, rCBV trends capturing temporal variation, or histograms identifying spatial variation, may be more descriptive and predictive. For instance, the paclitaxel study found that temporal changes in rCBV predicted lesion destiny, with rCBV trending downward

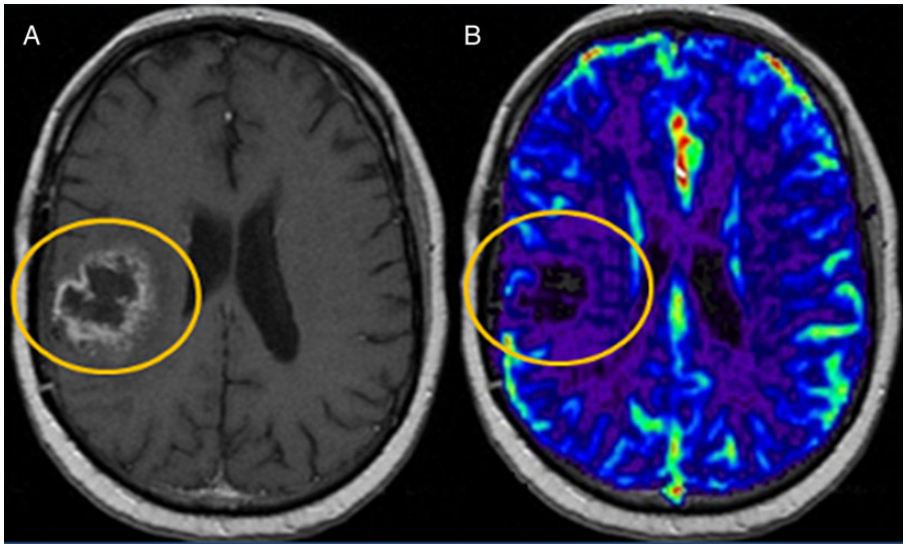

Fig. 7. Pseudoprogression and DSC-MRI. Contrast-enhanced axial T1-weighted MRI of a right-sided GBM shortly after temozolomide chemoradiation (A) demonstrates increased contrast enhancement suspicious for PD vs PsP. Color rCBV map from DSC-MRI (B) demonstrates low rCBV, consistent with PsP.

for PsP and upward for PD.[84] Histogram analysis of rCBV was used to study 79 GBM cases after progressive post-chemoradiation enhancement, and changes in histogram skewness and kurtosis predicted lesion destiny.[86] Similarly, fractional tumor volume using single-voxel rCBV thresholding with a cutoff of 1.0 has been shown to depict histologic tumor fraction in a study of 25 GBM tumors, and correlates with OS better than mean rCBV after progressive enhancement.[87] Trends in combined rCBV and ADC histograms between initial progressive enhancement and first subsequent follow-up were also used to study 35 GBM cases with progressive enhancement, and an increased population of low change in rCBV and high change in ADC on subtracted histograms predicted PsP, with the converse true for PD.[88] Emerging evidence therefore suggests that because of the complex pathophysiology of PsP and tendency for tumor and necrosis to coexist, rCBV analysis schemes that capture temporal (trends) and spatial (histogram) heterogeneity may have advantages over static measures of mean rCBV for distinguishing PsP and PD.

It is worth noting that multiple factors may impact reported literature results and threshold values of rCBV for distinguishing PsP from PD. These include mix of tumor grades; differences in chemoradiation; methods for confirming lesion destiny; variable DSC-MRI methodology, including acquisition parameters, preload and postprocessing leakage correction, and postprocessing software; timing of DSC-MRI in relation to initiation of chemoradiation; and data reduction strategies, including use of mean or median versus histograms or longitudinal trends. These sources for discrepancy emphasize the importance of careful consideration of methodological differences when adapting techniques from the literature, and the need for more imaging standardization.

DWI has also been investigated for differentiating PD from PsP, with the underlying assumption that PD will have higher cell density and lower corresponding ADC than PsP. ADC measured 2 months after completion of chemoradiation has shown promise in identifying PsP,[89] with high b-value acquisitions having potential benefit[90] in combination with ADC histogram analysis. However, DWI alone may not have sufficient accuracy for clinical decision making, and multimodal approaches including DWI may be beneficial,[91] with recent evidence[92] that volume-weighted voxel-based multiparametric clustering is more reproducible and accurate than single-parameter measurements for differentiating PsP from early PD in GBM. Several other groups have reported similar results.[93,94] The combination of MR spectroscopy, ADC, and rCBV has improved the discriminatory value of ADC alone.[95,96] Thus DWI may help improve the identification of PsP when used in combination with other physiologic imaging modalities; independently, its utility may be limited.

Another nascent application of PWI and DWI is the assessment of response to immunotherapy, which by virtue of induced inflammatory changes resulting in progressive contrast enhancement independent of tumor infiltration presents similar challenges to PsP.[97] These changes may actually portend a better prognosis and reflect response to treatment, rather than tumor progression. Importantly, the effectiveness of the immune response may take several weeks to manifest in healthy individuals, and potentially even longer in cancer patients with immunosuppression. Thus the time course of response may be patient specific and depend on the exact type of immunotherapy used. Preliminary evidence suggests that rCBV and ADC may have a role in assessing tumor burden in these patients. For instance, in a pilot study of 8 GBM tumors treated with dendritic cell immune therapy, high maximum rCBV and low minimum ADC were associated with tumor progression and were helpful for distinguishing inflammatory change associated with immune response from PD.[98] However, further investigation is required to confirm these results and to determine whether similar approaches to distinguish PsP from PD are translatable to other forms of immunotherapy.

Conclusion: General Recommendations, Standardization of Imaging for Brain Tumor Trials, and Emerging Imaging Methods

We have presented an overview of the principles of PWI and DWI and their application to response assessment and prognosis in patients with HGGs. Analysis methods of these functional techniques can vary, including: subjective/qualitative evaluation of parametric maps, user-defined ROI values (using mean, median, maximum, or minimum), histogram analysis, and voxel-wise analysis (ie, PRMs and fDMs). It should be noted that as universal quantitative imaging biomarker thresholds have not been established for various brain tumor applications, subjective/qualitative analysis is often used in the routine clinical setting. This is particularly true with rCBV maps, which are probably the most helpful problem-solving tool at this point, with good support in the literature.

While brain tumor imaging protocols vary widely across institutions, a few brief recommendations will be made with regard to PWI and DWI. We recommend the addition of at least DSC- and DWI-MRI to the standard contrast-enhanced MRI brain tumor protocol. For DSC-MRI, we recommend the use of a GBCA preload along with model-based postprocessing leakage correction for more accurate rCBV measurements. Longitudinal evaluation of rCBV from DSC-MRI can be especially helpful to identify active tumor.

However, it is clear that more technical standardization is required, particularly in the setting of multicenter brain tumor clinical trials.[99] For physiologic MRI techniques such as DWI and PWI, efforts related to technical standardization, including optimal acquisition parameters, postprocessing methods/software, determination of repeatability and reproducibility, and quality control methods are ongoing. Much preliminary evidence indicates the ability of advanced imaging, when judiciously applied, to improve assessment of tumor burden and treatment response in patients with recurrent glioblastoma. Solidifying evidence of clinical impact on decision making and future inclusion of these techniques in multicenter trials require sustained and focused efforts but could significantly improve the process of translating effective therapy from the laboratory to the clinic.

Lastly, emerging fields like *imaging genomics* may change the way in which physiologic MRI is utilized for brain tumor patient care. Perfusion and diffusion MRI metrics may have underlying genomic correlates. Integration of the imaging and genomic data may improve our understanding of tumor biology as well as be the source of novel prognostic, predictive, and early response imaging biomarkers in the near future.[100]

Funding

This work was supported in part by Southern California Clinical and Translational Science Institute (National Institutes of Health/National Center for Research Resources/National Center for Advancing Translational Sciences) grant no. KL2TR000131 to M.S.S.

Acknowledgments

The authors would like to thank Benjamin Ellingson, PhD, for providing material for some of the figures.

Conflicts of interest statement. M.S.S. is a consultant to Bayer, Guerbet. J.B.L. declares none. W.B.P. is a consultant to Roche, Amgen, Tocagen, and Celldex Therapeutics.

References

1. Shiroishi MS, Castellazzi G, Boxerman JL, et al. Principles of T2 *-weighted dynamic susceptibility contrast MRI technique in brain tumor imaging. *J Magn Reson Imaging*. 2015;41(2):296–313.
2. Essig M, Nguyen TB, Shiroishi MS, et al. Perfusion MRI: the five most frequently asked clinical questions. *AJR Am J Roentgenol*. 2013;201(3):W495–W510.
3. Essig M, Shiroishi MS, Nguyen TB, et al. Perfusion MRI: the five most frequently asked technical questions. *AJR Am J Roentgenol*. 2013;200(1):24–34.
4. Boxerman JL, Schmainda KM, Weisskoff RM. Relative cerebral blood volume maps corrected for contrast agent extravasation significantly correlate with glioma tumor grade, whereas uncorrected maps do not. *AJNR Am J Neuroradiol*. 2006;27(4):859–867.
5. Boxerman JL, Rosen BR, Weisskoff RM. Signal-to-noise analysis of cerebral blood volume maps from dynamic NMR imaging studies. *J Magn Reson Imaging*. 1997;7(3):528–537.
6. Welker K, Boxerman J, Kalnin A, et al. ASFNR recommendations for clinical performance of Mr dynamic susceptibility contrast perfusion imaging of the brain. *AJNR Am J Neuroradiol*. 2015;36(6):E41–E51.
7. Tofts PS, Brix G, Buckley DL, et al. Estimating kinetic parameters from dynamic contrast-enhanced T(1)-weighted MRI of a diffusable tracer: standardized quantities and symbols. *J Magn Reson Imaging*. 1999;10(3):223–232.
8. Ellingson BM, Malkin MG, Rand SD, et al. Validation of functional diffusion maps (fDMs) as a biomarker for human glioma cellularity. *J Magn Reson Imaging*. 2010;31(3):538–548.
9. Moffat BA, Chenevert TL, Lawrence TS, et al. Functional diffusion map: a noninvasive MRI biomarker for early stratification of clinical brain tumor response. *Proc Natl Acad Sci U S A*. 2005;102(15):5524–5529.
10. Ellingson BM, Cloughesy TF, Lai A, et al. Nonlinear registration of diffusion-weighted images improves clinical sensitivity of functional diffusion maps in recurrent glioblastoma treated with bevacizumab. *Magn Reson Med*. 2012;67(1):237–245.
11. Hirai T, Murakami R, Nakamura H, et al. Prognostic value of perfusion MR imaging of high-grade astrocytomas: long-term follow-up study. *AJNR Am J Neuroradiol*. 2008;29(8):1505–1510.
12. Jain R, Poisson L, Narang J, et al. Genomic mapping and survival prediction in glioblastoma: molecular subclassification strengthened by hemodynamic imaging biomarkers. *Radiology*. 2013;267(1):212–220.
13. Law M, Young RJ, Babb JS, et al. Gliomas: predicting time to progression or survival with cerebral blood volume measurements at dynamic susceptibility-weighted contrast-enhanced perfusion MR imaging. *Radiology*. 2008;247(2):490–498.
14. Zhang W, Kreisl T, Solomon J, et al. Acute effects of bevacizumab on glioblastoma vascularity assessed with DCE-MRI and relation to patient survival. *Paper presented at: Intl Soc Magn Reson Med2009*.

15. Bonekamp D, Deike K, Wiestler B, et al. Association of overall survival in patients with newly diagnosed glioblastoma with contrast-enhanced perfusion MRI: Comparison of intraindividually matched T1 - and T2 (*) -based bolus techniques. *J Magn Reson Imaging*. 2015;42(1):87–96.
16. Law M, Yang S, Babb JS, et al. Comparison of cerebral blood volume and vascular permeability from dynamic susceptibility contrast-enhanced perfusion MR imaging with glioma grade. *AJNR Am J Neuroradiol*. 2004;25(5):746–755.
17. Kickingereder P, Wiestler B, Graf M, et al. Evaluation of dynamic contrast-enhanced MRI derived microvascular permeability in recurrent glioblastoma treated with bevacizumab. *J Neurooncol*. 2015;121(2):373–380.
18. Nakamura H, Murakami R, Hirai T, et al. Can MRI-derived factors predict the survival in glioblastoma patients treated with postoperative chemoradiation therapy? *Acta Radiol*. 2013;54(2): 214–220.
19. Saraswathy S, Crawford FW, Lamborn KR, et al. Evaluation of MR markers that predict survival in patients with newly diagnosed GBM prior to adjuvant therapy. *J Neurooncol*. 2009;91(1):69–81.
20. Pope WB, Kim HJ, Huo J, et al. Recurrent glioblastoma multiforme: ADC histogram analysis predicts response to bevacizumab treatment. *Radiology*. 2009;252(1):182–189.
21. Pope WB, Qiao XJ, Kim HJ, et al. Apparent diffusion coefficient histogram analysis stratifies progression-free and overall survival in patients with recurrent GBM treated with bevacizumab: a multi-center study. *J Neurooncol*. 2012;108(3): 491–498.
22. Galanis E, Anderson SK, Lafky JM, et al. Phase II study of bevacizumab in combination with sorafenib in recurrent glioblastoma (N0776): a north central cancer treatment group trial. *Clin Cancer Res*. 2013;19(17):4816–4823.
23. Nagane M, Kobayashi K, Tanaka M, et al. Predictive significance of mean apparent diffusion coefficient value for responsiveness of temozolomide-refractory malignant glioma to bevacizumab: preliminary report. *Int J Clin Oncol*. 2014;19(1):16–23.
24. Wen Q, Jalilian L, Lupo JM, et al. Comparison of ADC metrics and their association with outcome for patients with newly diagnosed glioblastoma being treated with radiation therapy, temozolomide, erlotinib and bevacizumab. *J Neurooncol*. 2015; 121(2):331–339.
25. Pope WB, Lai A, Mehta R, et al. Apparent diffusion coefficient histogram analysis stratifies progression-free survival in newly diagnosed bevacizumab-treated glioblastoma. *AJNR Am J Neuroradiol*. 2011;32(5):882–889.
26. Hunter C, Smith R, Cahill DP, et al. A hypermutation phenotype and somatic MSH6 mutations in recurrent human malignant gliomas after alkylator chemotherapy. *Cancer Res*. 2006;66(8): 3987–3991.
27. Johnson BE, Mazor T, Hong C, et al. Mutational analysis reveals the origin and therapy-driven evolution of recurrent glioma. *Science*. 2014;343(6167):189–193.
28. van Thuijl HF, Mazor T, Johnson BE, et al. Evolution of DNA repair defects during malignant progression of low-grade gliomas after temozolomide treatment. *Acta Neuropathol*. 2015;129(4): 597–607.
29. Cao Y, Tsien CI, Nagesh V, et al. Survival prediction in high-grade gliomas by MRI perfusion before and during early stage of RT [corrected]. *Int J Radiat Oncol Biol Phys*. 2006;64(3):876–885.
30. Bag AK, Cezayirli PC, Davenport JJ, et al. Survival analysis in patients with newly diagnosed primary glioblastoma multiforme using pre- and post-treatment peritumoral perfusion imaging parameters. *J Neurooncol*. 2014;120(2):361–370.
31. Mangla R, Singh G, Ziegelitz D, et al. Changes in relative cerebral blood volume 1 month after radiation-temozolomide therapy can help predict overall survival in patients with glioblastoma. *Radiology*. 2010;256(2):575–584.
32. Hamstra DA, Chenevert TL, Moffat BA, et al. Evaluation of the functional diffusion map as an early biomarker of time-to-progression and overall survival in high-grade glioma. *Proc Natl Acad Sci U S A*. 2005;102(46):16759–16764.
33. Lee KC, Bradley DA, Hussain M, et al. A feasibility study evaluating the functional diffusion map as a predictive imaging biomarker for detection of treatment response in a patient with metastatic prostate cancer to the bone. *Neoplasia*. 2007;9(12):1003–1011.
34. Moffat BA, Chenevert TL, Meyer CR, et al. The functional diffusion map: an imaging biomarker for the early prediction of cancer treatment outcome. *Neoplasia*. 2006;8(4):259–267.
35. Galban CJ, Chenevert TL, Meyer CR, et al. The parametric response map is an imaging biomarker for early cancer treatment outcome. *Nat Med*. 2009;15(5):572–576.
36. Lemasson B, Chenevert TL, Lawrence TS, et al. Impact of perfusion map analysis on early survival prediction accuracy in glioma patients. *Transl Oncol*. 2013;6(6):766–774.
37. Hamstra DA, Galban CJ, Meyer CR, et al. Functional diffusion map as an early imaging biomarker for high-grade glioma: correlation with conventional radiologic response and overall survival. *J Clin Oncol*. 2008;26(20):3387–3394.
38. Ellingson BM, Cloughesy TF, Lai A, et al. Quantitative probabilistic functional diffusion mapping in newly diagnosed glioblastoma treated with radiochemotherapy. *Neuro Oncol*. 2013;15(3): 382–390.
39. Ellingson BM, Cloughesy TF, Zaw T, et al. Functional diffusion maps (fDMs) evaluated before and after radiochemotherapy predict progression-free and overall survival in newly diagnosed glioblastoma. *Neuro Oncol*. 2012;14(3):333–343.
40. Hiramatsu R, Kawabata S, Furuse M, et al. Identification of early and distinct glioblastoma response patterns treated by boron neutron capture therapy not predicted by standard radiographic assessment using functional diffusion map. *Radiat Oncol*. 2013;8(1):192.
41. McConville P, Hambardzumyan D, Moody JB, et al. Magnetic resonance imaging determination of tumor grade and early response to temozolomide in a genetically engineered mouse model of glioma. *Clin Cancer Res*. 2007;13(10):2897–2904.
42. Lemasson B, Galban CJ, Boes JL, et al. Diffusion-weighted MRI as a biomarker of tumor radiation treatment response heterogeneity: a comparative study of whole-volume histogram analysis versus voxel-based functional diffusion map analysis. *Transl Oncol*. 2013;6(5):554–561.
43. Sawlani RN, Raizer J, Horowitz SW, et al. Glioblastoma: a method for predicting response to antiangiogenic chemotherapy by using MR perfusion imaging—pilot study. *Radiology*. 2010;255(2): 622–628.
44. Verhoeff JJ, Lavini C, van Linde ME, et al. Bevacizumab and dose-intense temozolomide in recurrent high-grade glioma. *Ann Oncol*. 2010;21(8):1723–1727.
45. Schmainda KM, Prah M, Connelly J, et al. Dynamic-susceptibility contrast agent MRI measures of relative cerebral blood volume predict response to bevacizumab in recurrent high-grade glioma. *Neuro Oncol*. 2014;16(6):880–888.

46. Leu K, Enzmann DR, Woodworth DC, et al. Hypervascular tumor volume estimated by comparison to a large-scale cerebral blood volume radiographic atlas predicts survival in recurrent glioblastoma treated with bevacizumab. *Cancer Imaging*. 2014; 14:31.
47. Schmainda KM, Zhang Z, Prah M, et al. Dynamic susceptibility contrast MRI measures of relative cerebral blood volume as a prognostic marker for overall survival in recurrent glioblastoma: results from the ACRIN 6677/RTOG 0625 multicenter trial. *Neuro Oncol*. 2015;17(8):1148–1156.
48. Rahman R, Hamdan A, Zweifler R, et al. Histogram analysis of apparent diffusion coefficient within enhancing and nonenhancing tumor volumes in recurrent glioblastoma patients treated with bevacizumab. *J Neurooncol*. 2014;119(1): 149–158.
49. Ellingson BM, Cloughesy TF, Lai A, et al. Graded functional diffusion map-defined characteristics of apparent diffusion coefficients predict overall survival in recurrent glioblastoma treated with bevacizumab. *Neuro Oncol*. 2011;13(10): 1151–1161.
50. Ellingson BM, Cloughesy TF, Lai A, et al. Cell invasion, motility, and proliferation level estimate (CIMPLE) maps derived from serial diffusion MR images in recurrent glioblastoma treated with bevacizumab. *J Neurooncol*. 2011;105(1):91–101.
51. Khayal IS, Polley MY, Jalbert L, et al. Evaluation of diffusion parameters as early biomarkers of disease progression in glioblastoma multiforme. *Neuro Oncol*. 2010;12(9):908–916.
52. Gilbert MR, Dignam JJ, Armstrong TS, et al. A randomized trial of bevacizumab for newly diagnosed glioblastoma. *N Engl J Med*. 2014;370(8):699–708.
53. Norden AD, Drappatz J, Muzikansky A, et al. An exploratory survival analysis of anti-angiogenic therapy for recurrent malignant glioma. *J Neurooncol*. 2009;92(2):149–155.
54. Ellingson BM, Cloughesy TF, Lai A, et al. Quantitative volumetric analysis of conventional MRI response in recurrent glioblastoma treated with bevacizumab. *Neuro Oncol*. 2011; 13(4):401–409.
55. Wen PY, Macdonald DR, Reardon DA, et al. Updated response assessment criteria for high-grade gliomas: response assessment in neuro-oncology working group. *J Clin Oncol*. 2010;28(11):1963–1972.
56. Boxerman JL, Zhang Z, Safriel Y, et al. Early post-bevacizumab progression on contrast-enhanced MRI as a prognostic marker for overall survival in recurrent glioblastoma: results from the ACRIN 6677/RTOG 0625 Central Reader Study. *Neuro Oncol*. 2013;15(7):945–954.
57. Boxerman JL, Zhang Z, Schmainda KM, et al. Early post-bevacizumab change in rCBV from DSC-MRI predicts overall survival in recurrent glioblastoma whereas 2D-T1 response status does not: results from the ACRIN 6677/RTOG 0625 multi-center study. *Paper presented at: Radiological Society of North America 100th Scientific Assembly 2014*; Chicago.
58. Artzi M, Bokstein F, Blumenthal DT, et al. Differentiation between vasogenic-edema versus tumor-infiltrative area in patients with glioblastoma during bevacizumab therapy: a longitudinal MRI study. *Eur J Radiol*. 2014;83(7):1250–1256.
59. Artzi M, Blumenthal DT, Bokstein F, et al. Classification of tumor area using combined DCE and DSC MRI in patients with glioblastoma. *J Neurooncol*. 2015;121(2):349–357.
60. Akbari H, Macyszyn L, Da X, et al. Pattern analysis of dynamic susceptibility contrast-enhanced MR imaging demonstrates peritumoral tissue heterogeneity. *Radiology*. 2014;273(2): 502–510.
61. Jain R, Poisson LM, Gutman D, et al. Outcome prediction in patients with glioblastoma by using imaging, clinical, and genomic biomarkers: focus on the nonenhancing component of the tumor. *Radiology*. 2014;272(2):484–493.
62. Gerstner ER, Chen PJ, Wen PY, et al. Infiltrative patterns of glioblastoma spread detected via diffusion MRI after treatment with cediranib. *Neuro Oncol*. 2010;12(5):466–472.
63. Gerstner ER, Frosch MP, Batchelor TT. Diffusion magnetic resonance imaging detects pathologically confirmed, nonenhancing tumor progression in a patient with recurrent glioblastoma receiving bevacizumab. *J Clin Oncol*. 2010;28(6): e91–e93.
64. Lutz K, Wiestler B, Graf M, et al. Infiltrative patterns of glioblastoma: identification of tumor progress using apparent diffusion coefficient histograms. *J Magn Reson Imaging*. 2014; 39(5):1096–1103.
65. Gupta A, Young RJ, Karimi S, et al. Isolated diffusion restriction precedes the development of enhancing tumor in a subset of patients with glioblastoma. *AJNR Am J Neuroradiol*. 2011;32(7): 1301–1306.
66. Takano S, Kimu H, Tsuda K, et al. Decrease in the apparent diffusion coefficient in peritumoral edema for the assessment of recurrent glioblastoma treated by bevacizumab. *Acta Neurochir Suppl*. 2013;118:185–189.
67. Farid N, Almeida-Freitas DB, White NS, et al. Restriction-spectrum imaging of bevacizumab-related necrosis in a patient with GBM. *Front Oncol*. 2013;3:258.
68. LaViolette PS, Mickevicius NJ, Cochran EJ, et al. Precise ex vivo histological validation of heightened cellularity and diffusion-restricted necrosis in regions of dark apparent diffusion coefficient in 7 cases of high-grade glioma. *Neuro Oncol*. 2014;16(12):1599–1606.
69. Rieger J, Bahr O, Muller K, et al. Bevacizumab-induced diffusion-restricted lesions in malignant glioma patients. *J Neurooncol*. 2010;99(1):49–56.
70. Mong S, Ellingson BM, Nghiemphu PL, et al. Persistent diffusion-restricted lesions in bevacizumab-treated malignant gliomas are associated with improved survival compared with matched controls. *AJNR Am J Neuroradiol*. 2012;33(9): 1763–1770.
71. Sivasundaram L, Hazany S, Wagle N, et al. Diffusion restriction in a non-enhancing metastatic brain tumor treated with bevacizumab—recurrent tumor or atypical necrosis? *Clin Imaging*. 2014;38(5):724–726.
72. Futterer SF, Nemeth AJ, Grimm SA, et al. Diffusion abnormalities of the corpus callosum in patients receiving bevacizumab for malignant brain tumors: suspected treatment toxicity. *J Neurooncol*. 2014;118(1):147–153.
73. Brandsma D, Stalpers L, Taal W, et al. Clinical features, mechanisms, and management of pseudoprogression in malignant gliomas. *Lancet Oncol*. 2008;9(5):453–461.
74. Young RJ, Gupta A, Shah AD, et al. Potential utility of conventional MRI signs in diagnosing pseudoprogression in glioblastoma. *Neurology*. 2011;76(22):1918–1924.
75. Sugahara T, Korogi Y, Tomiguchi S, et al. Posttherapeutic intraaxial brain tumor: the value of perfusion-sensitive contrast-enhanced MR imaging for differentiating tumor

recurrence from nonneoplastic contrast-enhancing tissue. *AJNR Am J Neuroradiol*. 2000;21(5):901–909.

76. Barajas RF Jr., Chang JS, Segal MR, et al. Differentiation of recurrent glioblastoma multiforme from radiation necrosis after external beam radiation therapy with dynamic susceptibility-weighted contrast-enhanced perfusion MR imaging. *Radiology*. 2009;253(2):486–496.
77. Gasparetto EL, Pawlak MA, Patel SH, et al. Posttreatment recurrence of malignant brain neoplasm: accuracy of relative cerebral blood volume fraction in discriminating low from high malignant histologic volume fraction. *Radiology*. 2009;250(3): 887–896.
78. Tsien C, Galban CJ, Chenevert TL, et al. Parametric response map as an imaging biomarker to distinguish progression from pseudoprogression in high-grade glioma. *J Clin Oncol*. 2010; 28(13):2293–2299.
79. Prager AJ, Martinez N, Beal K, et al. Diffusion and perfusion MRI to differentiate treatment-related changes including pseudoprogression from recurrent tumors in high-grade gliomas with histopathologic evidence. *AJNR Am J Neuroradiol*. 2015;36(5):877–885.
80. Young RJ, Gupta A, Shah AD, et al. MRI perfusion in determining pseudoprogression in patients with glioblastoma. *Clin Imaging*. 2013;37(1):41–49.
81. Kong DS, Kim ST, Kim EH, et al. Diagnostic dilemma of pseudoprogression in the treatment of newly diagnosed glioblastomas: the role of assessing relative cerebral blood flow volume and oxygen-6-methylguanine-DNA methyltransferase promoter methylation status. *AJNR Am J Neuroradiol*. 2011; 32(2):382–387.
82. Gahramanov S, Raslan AM, Muldoon LL, et al. Potential for differentiation of pseudoprogression from true tumor progression with dynamic susceptibility-weighted contrast-enhanced magnetic resonance imaging using ferumoxytol vs. gadoteridol: a pilot study. *Int J Radiat Oncol Biol Phys*. 2011; 79(2):514–523.
83. Gahramanov S, Muldoon LL, Varallyay CG, et al. Pseudoprogression of glioblastoma after chemo- and radiation therapy: diagnosis by using dynamic susceptibility-weighted contrast-enhanced perfusion MR imaging with ferumoxytol versus gadoteridol and correlation with survival. *Radiology*. 2013;266(3):842–852.
84. Boxerman JL, Ellingson BM, Jeyapalan S, et al. Longitudinal DSC-MRI for distinguishing tumor recurrence from pseudoprogression in patients with a high-grade glioma. *Am J Clin Oncol*. 2014;Nov 26 [Epub ahead of print].
85. Di Chiro G, Oldfield E, Wright DC, et al. Cerebral necrosis after radiotherapy and/or intraarterial chemotherapy for brain tumors: PET and neuropathologic studies. *AJR Am J Roentgenol*. 1988;150(1):189–197.
86. Baek HJ, Kim HS, Kim N, et al. Percent change of perfusion skewness and kurtosis: a potential imaging biomarker for early treatment response in patients with newly diagnosed glioblastomas. *Radiology*. 2012;264(3):834–843.
87. Hu LS, Eschbacher JM, Heiserman JE, et al. Reevaluating the imaging definition of tumor progression: perfusion MRI quantifies recurrent glioblastoma tumor fraction, pseudoprogression, and radiation necrosis to predict survival. *Neuro Oncol*. 2012;14(7):919–930.
88. Cha J, Kim ST, Kim HJ, et al. Differentiation of tumor progression from pseudoprogression in patients with posttreatment glioblastoma using multiparametric histogram analysis. *AJNR Am J Neuroradiol*. 2014;35(7):1309–1317.
89. Lee WJ, Choi SH, Park CK, et al. Diffusion-weighted MR imaging for the differentiation of true progression from pseudoprogression following concomitant radiotherapy with temozolomide in patients with newly diagnosed high-grade gliomas. *Acad Radiol*. 2012;19(11):1353–1361.
90. Chu HH, Choi SH, Ryoo I, et al. Differentiation of true progression from pseudoprogression in glioblastoma treated with radiation therapy and concomitant temozolomide: comparison study of standard and high-b-value diffusion-weighted imaging. *Radiology*. 2013;269(3):831–840.
91. Kalpathy-Cramer J, Gerstner ER, Emblem KE, et al. Advanced magnetic resonance imaging of the physical processes in human glioblastoma. *Cancer Res*. 2014;74(17):4622–4637.
92. Park JE, Kim HS, Goh MJ, et al. Pseudoprogression in patients with glioblastoma: assessment by using volume-weighted voxel-based multiparametric clustering of mr imaging data in an independent test set. *Radiology*. 2015;275(3):792–802.
93. Kim HS, Goh MJ, Kim N, et al. Which combination of MR imaging modalities is best for predicting recurrent glioblastoma? Study of diagnostic accuracy and reproducibility. *Radiology*. 2014;273(3): 831–843.
94. Song YS, Choi SH, Park CK, et al. True progression versus pseudoprogression in the treatment of glioblastomas: a comparison study of normalized cerebral blood volume and apparent diffusion coefficient by histogram analysis. *Korean J Radiol*. 2013;14(4):662–672.
95. Di Costanzo A, Scarabino T, Trojsi F, et al. Recurrent glioblastoma multiforme versus radiation injury: a multiparametric 3-T MR approach. *Radiol Med*. 2014;119(8):616–624.
96. Matsusue E, Fink JR, Rockhill JK, et al. Distinction between glioma progression and post-radiation change by combined physiologic MR imaging. *Neuroradiology*. 2010;52(4):297–306.
97. Huang RY, Neagu MR, Reardon DA, Wen PY. Pitfalls in the neuroimaging of glioblastoma in the era of antiangiogenic and immuno/targeted therapy - detecting illusive disease, defining response. *Front Neurol*. 2015;6:33.
98. Vrabec M, Van Cauter S, Himmelreich U, et al. MR perfusion and diffusion imaging in the follow-up of recurrent glioblastoma treated with dendritic cell immunotherapy: a pilot study. *Neuroradiology*. 2011;53(10):721–731.
99. Wen PY, Cloughesy TF, Ellingson BM, et al. Report of the Jumpstarting Brain Tumor Drug Development Coalition and FDA clinical trials neuroimaging endpoint workshop (January 30, 2014, Bethesda MD). *Neuro Oncol*. 2014;16(Suppl 7): vii36–vii47.
100. Pope WB. Genomics of brain tumor imaging. *Neuroimaging Clin N Am*. 2015;25(1):105–119.